Complex amplitudes tracking loop for multipath slow fading channel estimation in OFDM systems

Laurent Ros, Hussein Hijazi, Eric Pierre Simon

Complex amplitudes tracking loop for multipath slow fading channel estimation in OFDM systems

Laurent ROS[1], Hussein HIJAZI[2] and Eric-Pierre SIMON[2]

April 13, 2012,
Research Report (technical note) of the Gipsa-lab laboratory

1: GIPSA-lab, Image and Signal Department, BP 46 - 38402 Saint Martin d'Hères - FRANCE
2: Lebanese International University (LIU), Beirut, LEBANON
3: IEMN lab, TELICE group, 59655 Villeneuve d'Ascq, University of Lille, FRANCE
E-mail: laurent.ros@gipsa-lab.inpg.fr, hijazi.hussein@liu.edu.lb, eric.simon@univ-lille1.fr

Abstract

This Gipsa-lab research report[1] deals with channel estimation for Orthogonal Frequency Division Multiplexing systems over slowly-varying multi-path fading channels. Most of the conventional methods exploit the frequency-domain correlation in estimating the channel at pilot subcarriers position, and then interpolating it over the entire frequency grid. More advanced algorithms exploit the time-domain correlation as well, by employing Kalman filter based on the approximation of the time-varying (assumed Rayleigh with Jakes'spectrum) channel. Adopting a parametric approach and assuming a primary acquisition of delay related information, channel estimator has to track the Complex Amplitudes (CAs) of the channel paths. In this perspective, we propose a reduced complexity algorithm compared to Kalman methods, based on a second-order CA Tracking Loop. Inspired by Phase-Locked Loops, an error signal is built from the pilot-aided Least-Squares (LS) estimate of the CAs, and is integrated by the loop to carry out the final CAs estimate. We derive closed-form expressions of the Mean Square Error (MSE) of the algorithm, and of the corresponding optimal loop coefficients. Simulation results show that our algorithm outperforms the conventional (frequency-domain interpolation) method and has almost the same performance as a second-order Kalman based algorithm. Moreover, efficiency of a second-order versus first-order approach is demonstrated for the slow-fading case, with a MSE closer to the Bayesian-Cramer-Rao-Bound.

Index Terms

OFDM, Channel estimation, Rayleigh multi-path channel, Jakes'spectrum, Tracking Loop, Phase Locked Loop, Kalman filter, Auto-Regressive model.

I. Introduction

Orthogonal Frequency Division Multiplexing (OFDM) is an effective technique for alleviating frequency-selective channel effects in wireless communication systems. In this technique, a wideband frequency-selective channel is converted to a number of parallel narrow-band flat fading subchannels which are free of Intersymbol Interference (ISI) and free (assuming negligible channel time variation within one OFDM symbol period T) of Inter-Carrier Interference (ICI). For coherent detection of the information symbols, reliable estimation of the gain of each subchannel in the OFDM system is crucial.

A. Some approaches to channel estimation in OFDM

Most of the conventional methods work in a symbol-by-symbol scheme [1] [2] [3] by using the correlation of the channel only in the frequency-domain (FD), $i.e.$ the correlation between subchannels. Generally, they consist of estimating the channel at pilot frequencies and then interpolating the channel frequency response [1]. The channel estimation at the pilot frequencies can be based on the Least-Squares (LS) criterion, or for better performance on the Linear-Minimum-Mean-Square-Error (LMMSE) criterion [2]. In [3], Low-Pass Interpolation (LPI) has been shown to perform better than all interpolation techniques used in channel estimation.

[1]The final revised form of this paper was written November 15, 2010 (after an initial version on July 14th 2010), and a part of this work was presented in the conference [18] (ISCCSP, Limassol, Cyprus, March 2010). The goal of the on-line posting of this manuscript is to provide analytical results about the so-called *first algorithm* proposed in [18].

Though the conventional methods can operate with time-varying channels, the information of the time-domain correlation is not exploited. However, we have shown in [4] through on-line Bayesian Cramer-Rao-Bound (BCRB) analysis, how much the channel estimation process of the current symbol can be improved by using the previous OFDM symbols. Some works have addressed the time-domain dynamics of the fading process to obtain an updated channel estimate. Chen and Zhang proposed in [5] a structure which uses a Kalman filter estimator for each subchannel (exploits the time-domain correlation) and a linear combiner to refine the estimate of each subchannel (exploits the frequency-domain correlation). The complexity of the proposed structure increases with the number of subcarriers. However in practice, only a subset of (pilot) subcarriers can be used to perform the per-subchannel Kalman filter, and the global frequency response of the channel can still be obtained by LPI interpolation. Other works using Kalman filter to exploit time and frequency correlation for OFDM channel estimation are based on additional assumptions or different approaches. Assuming the availability of the power delay profile, a data-aided Kalman estimator (derived from the Expectation-Maximization algorithm framework) is employed in [6] to track the discrete-time impulse response of the channel ($i.e$ in Time-Domain (TD)). And a low-complexity parameter reduction approach based on the eigenvalues decomposition of the auto-correlation matrix of the channel (in FD) is proposed in [7]. It tracks the channel coefficients in the dominant eigenvectors subspace basis, before performing eigenvalues interpolation to compute the channel frequency response.

In the same idea of reducing the signal subspace dimension, we now focus on the class of parametric channel estimator [8] [9]. Assuming a multi-path channel structure, estimation can be reduced to the estimation of certain physical propagation parameters, such as multi-path delays and multi-path Complex Amplitudes (CAs) [8] [10] [11] [12], summarized in an L-path channel structure. Moreover, in wireless radio channels, the CAs show temporal variations while the delays are quasi-constant over a large number of OFDM symbols, and then can be accurately estimated by an acquisition procedure. In [8], the acquisition includes the detection of the number of paths based on the MDL (Maximum Description Length) principle and the acquisition of the initial multipath time delays through the ESPRIT (Estimation of Signal Parameters by Rotational Invariance Techniques) method. With this information, a MMSE estimator is derived to estimate the channel frequency response, with a great performance compared to non-parametric methods. However, the optimal Wiener estimator remains complex and requires the knowledge of the second-order statistical properties of the channel. In [10], the delay-subspace (assumed invariant over several symbols) and the fast variation of the CAs are tracked separately by subspace-tracking algorithms. In [11] [12], we have addressed the problem of paths CA estimation and ICI reduction for the case of fast-varying Rayleigh channel (normalized Doppler spread $f_dT \geq 10^{-2}$). Based on a polynomial modeling of the (Jakes process) CA variation, we used polynomial estimation over a block of OFDM symbols in [11], and a Kalman filter based on Auto-regressive (AR) model of the polynomial coefficients dynamic in [12].

B. Motivation of the work and contributions

The use of Kalman filters for the channel estimation problem has received great attention in recent years in the wireless communication literature. Various approaches have been developed, as mentioned in the previous examples [5] [6] [7] [12], and not only of course for OFDM systems [15]. All the aforementioned works based their Kalman filter on the AR approximation of the widely accepted Rayleigh fading channel with Jakes'Doppler spectrum [24], as developed in [13]. The first-order Gauss-Markov assumption (AR1 model) is often retained [14] [25] [6] [7] [15] [16]. However, the so-called AR1-Kalman estimator does not ensure to reach the BCRB in the much common scenario of slowly varying channel ($i.e.$ when ICI is negligible) [17] [18]. Moreover, and above all, the AR1-Kalman is still a quite complex algorithm even if it employs only a first-order state-space model.

In this paper, we propose a simplified on-line recursive algorithm for the multi-path CAs estimation problem under the slow channel variations scenario ($f_dT \leq 10^{-2}$). It is developed for OFDM systems into the class of parametric channel estimators, exploiting the availability of delay related information (assuming a primary acquisition procedure as in [8] [11] [12]) for tracking the CA variations. But, it could be also directly applied to the more basic single-carrier flat fading channel estimation problem, or adapted for other approaches than parametric approach. Our main motivations for the work presented in this paper are the following:

- to obtain a reduced complexity algorithm compared to Kalman filter based algorithms, with quasi same asymptotic MSE performance (for a same model order),

- to obtain a closed-form and usable expression of the performance in MSE with respect to the channel state (Doppler spread, power-delay profile, SNR), derived from theoretical analysis under "Rayleigh-Jakes" assumption.
- to measure the advantage of choosing a proper 2nd-order model to approach slow fading variation, versus a first-order model.

The proposed algorithms is based on a Complex Amplitudes Tracking Loop (CATL) structure. This structure is inspired by the "prediction-correction" principle of the Kalman filter [30], and by second-order digital Phase-Locked Loops (PLL) [19] [22] [26]. Therefore, *increments* (or *drifts*) into the CAs variations are also estimated in order to improve the CAs prediction for the next iteration, exploiting the time-domain correlation and especially the fact that CAs exhibit strong trend behavior ($i.e.$ they continue in some direction during several OFDM symbols). The error signal that feeds the loop is based on the (per current symbol) LS estimate of the paths CA, obtained from the pilot-subcarriers. A theoretical analysis of the CATL combined with this specific error signal (leading to the proposed LS-CATL algorithm) is derived. Three natural references (the AR1-Kalman filter, a 2nd-order Kalman filter, and the BCRB) useful to appreciate the MSE of our algorithm with the same (parametric modeling) assumptions are also presented. Simulation results compared to these obvious references and also to other literature algorithms validate the proposed algorithm and the theoretical analysis.

The paper is organized as follows: Section II describes the system model. Section III derives the two suboptimal algorithms, whereas Section IV recalls the Kalman algorithm and the BCRB references. Finally, the different results are discussed in Section V.

Notations: $[\mathbf{x}]_k$ denotes the kth entry of the vector $\mathbf{x}$, and $[\mathbf{X}]_{k,m}$ the $[k,m]$th entry of the matrix $\mathbf{X}$ (indices begin from 1). $\mathbf{I}_N$ is a $N \times N$ identity matrix. The notation diag$\{\mathbf{x}\}$ stands for a diagonal matrix with $\mathbf{x}$ on its diagonal, diag$\{\mathbf{X}\}$ is a vector whose elements are the elements of the diagonal of $\mathbf{X}$, and blkdiag$\{\mathbf{X},\mathbf{Y}\}$ is a block diagonal matrix with the matrices $\mathbf{X}$ and $\mathbf{Y}$ on its diagonal. The superscripts $(\cdot)^T$, $(\cdot)^H$, $|\cdot|$, and Tr$(\cdot)$ stand respectively for transpose and Hermitian operators, determinant and trace operations. $J_0(\cdot)$ is the zeroth-order Bessel function of the first kind. $\nabla_{\mathbf{x}}$ represents the first partial derivatives operator $i.e.$, $\nabla_{\mathbf{x}} = [\frac{\partial}{\partial x_1}, ..., \frac{\partial}{\partial x_N}]^T$.

II. System Model

A. OFDM Transmission over multi-path channel

Consider an OFDM system with N sub-carriers, and a cyclic prefix length N_g. The duration of an OFDM symbol is $T = vT_s$, where T_s is the sampling time and $v = N+N_g$. Let $\mathbf{x}_{(n)} = \left[x_{(n)}[-\frac{N}{2}], x_{(n)}[-\frac{N}{2}+1], ..., x_{(n)}[\frac{N}{2}-1]\right]^T$ be the nth transmitted OFDM symbol, where $\{x_{(n)}[b]\}$ are normalized QAM symbols. After transmission over a multi-path channel and FFT demodulation, the nth received OFDM symbol $\mathbf{y}_{(n)} = \left[y_{(n)}[-\frac{N}{2}], y_{(n)}[-\frac{N}{2}+1], ..., y_{(n)}[\frac{N}{2}-1]\right]^T$ is given by [8] [11]:

$$\mathbf{y}_{(n)} \;=\; \mathbf{H}_{(n)}\ \mathbf{x}_{(n)} + \mathbf{w}_{(n)} \tag{1}$$

where $\mathbf{w}_{(n)}$ is a $N \times 1$ zero-mean complex circular Gaussian noise vector with covariance matrix $\sigma^2\mathbf{I}_N$, and $\mathbf{H}_{(n)}$ is a $N \times N$ diagonal matrix with diagonal elements given by

$$[\mathbf{H}_{(n)}]_{k,k} = \frac{1}{N}\sum_{l=1}^{L}\left[\alpha_{l(n)} \times e^{-j2\pi(\frac{k-1}{N}-\frac{1}{2})\tau_l}\right] \tag{2}$$

L is the total number of propagation paths, α_l is the lth CA of variance $\sigma^2_{\alpha_l}$ (with $\sum_{l=1}^{L}\sigma^2_{\alpha_l} = 1$), and $\tau_l \times T_s$ is the lth delay (τ_l is not necessarily an integer, but $\tau_L < N_g$). The L individual elements of $\{\alpha_{l(n)}\}$ are uncorrelated with respect to each other. Using (2), the observation model in (1) for the nth OFDM symbol can be re-written as

$$\mathbf{y}_{(n)} \;=\; \text{diag}\{\mathbf{x}_{(n)}\}\mathbf{F}\ \boldsymbol{\alpha}_{(n)} + \mathbf{w}_{(n)} \tag{3}$$

where $\boldsymbol{\alpha}_{(n)} = [\alpha_{1(n)}, ..., \alpha_{L(n)}]^T$ and $\mathbf{F}$ is a $N \times L$ Fourier matrix depending on the delays distribution, defined by [8]:

$$[\mathbf{F}]_{k,l} = e^{-j2\pi(\frac{k-1}{N}-\frac{1}{2})\tau_l} \tag{4}$$

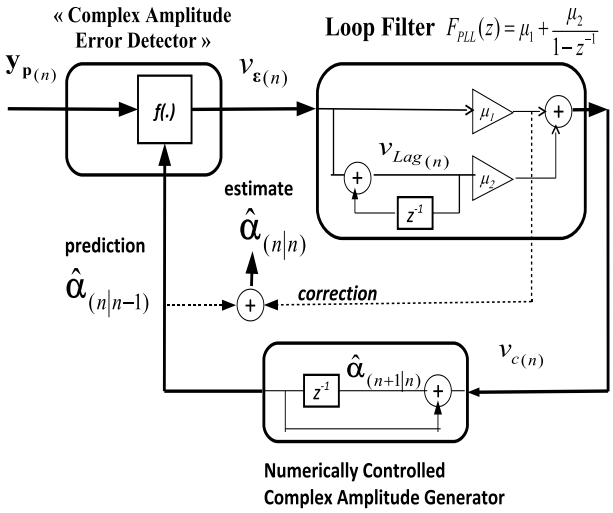

Fig. 1. Equivalent structure of the second-order complex amplitude tracking loop, inspired by second-order digital PLL

The algorithm proposed in this paper can work without explicit *a priori* model for the paths CA variation. However, we will provide theoretical expressions for the case of the widely accepted Rayleigh model with the so-called Jakes' power spectrum [24] with Doppler frequency f_d, named "Rayleigh-Jakes" model in this paper. It means that the L CA $\alpha_{l(n)}$ are independent wide-sense stationary narrow-band zero-mean complex circular Gaussian processes, with correlation coefficients for a time-lag p given by

$$\mathrm{R}_{\alpha_l}^{(p)} = \mathrm{E}[\alpha_{l(n)}{\alpha_{l(n-p)}}^H] \quad = \quad \sigma_{\alpha_l}^2 J_0(2\pi f_d T p) \tag{5}$$

B. Pilot Pattern

The N_p pilot subcarriers are evenly inserted into the N subcarriers at the positions $\mathcal{P} = \{p_s \mid p_s = (s-1)L_f + 1,\ s = 1, ..., N_p\}$ with L_f the distance between two adjacent pilots. The received pilot subcarriers can be written as

$$\mathbf{y}_{\mathbf{p}(n)} \quad = \quad \boldsymbol{\mathcal{K}}_{(n)}\boldsymbol{\alpha}_{(n)} + \mathbf{w}_{\mathbf{p}(n)} \tag{6}$$

where $\mathbf{y_p}$ and $\mathbf{w_p}$ are $N_p \times 1$ vectors, and where we have defined the $N_p \times L$ matrix

$$\boldsymbol{\mathcal{K}}_{(n)} = \mathrm{diag}\{\mathbf{x}_{\mathbf{p}(n)}\}\mathbf{F_p} \tag{7}$$

that can be computed for each symbol period n from the knowledge of the $N_p \times 1$ data pilot vector $\mathbf{x}_{\mathbf{p}(n)}$ and the delays $\{\tau_l\}$ through the $N_p \times L$ Fourier transform matrix $\mathbf{F_p}$ with elements given by

$$[\mathbf{F_p}]_{k,l} = e^{-j2\pi(\frac{p_k-1}{N}-\frac{1}{2})\tau_l} \tag{8}$$

III. Complex Amplitude Tracking Algorithm

The proposed tracking algorithm, called LS based-CATL algorithm, is built from a general second-order recursive structure (CATL), and a specific error signal (based on LS criterion) that conditions one element of the structure.

A. Structure of the algorithm: CA Tracking Loop

1) Structure: The purpose is to estimate the channel coefficients $\boldsymbol{\alpha}$. The estimate of $\boldsymbol{\alpha}_{(n)}$, denoted $\hat{\boldsymbol{\alpha}}_{(n|n)}$, is updated at a symbol rate by the computation of a loop error signal $\boldsymbol{v}_{\boldsymbol{\epsilon}(n)}$, which is next filtered by a digital loop filter. Inspired by the Phase-Locked-Loop (PLL) design [26], we use a second-order closed-loop to get the ability to track potential time linear drifts of the parameters to be estimated. The general recursive equations can be given

by the way of two stages:

Measurement Update Equations

$$\boldsymbol{v}_{\boldsymbol{\epsilon}(n)} = function\ of\ \{\ \mathbf{y}_{\mathbf{p}(n)}; \hat{\boldsymbol{\alpha}}_{(n|n-1)}\ \} \quad (9)$$

$$\hat{\boldsymbol{\alpha}}_{(n|n)} = \hat{\boldsymbol{\alpha}}_{(n|n-1)} + \mu_1.\boldsymbol{v}_{\boldsymbol{\epsilon}(n)} \quad (10)$$

Time Update equations

$$\boldsymbol{v}_{\mathbf{Lag}(n)} = \boldsymbol{v}_{\mathbf{Lag}(n-1)} + \boldsymbol{v}_{\boldsymbol{\epsilon}(n)} \quad (11)$$

$$\hat{\boldsymbol{\alpha}}_{(n+1|n)} = \hat{\boldsymbol{\alpha}}_{(n|n)} + \mu_2.\boldsymbol{v}_{\mathbf{Lag}(n)} \quad (12)$$

where μ_1, μ_2 are the (real positive) loop coefficients.

As in a Kalman filter, the Time Update Equations can be thought of predictor equations, while the Measurement Update Equations can be thought of corrector equations.

The Measurement Update Equations are responsible for the feedback, $i.e.$, for incorporating a new measurement $\mathbf{y}_{\mathbf{p}(n)}$ into the *a priori* estimate $\hat{\boldsymbol{\alpha}}_{(n|n-1)}$ to obtain an improved *a posteriori* estimate $\hat{\boldsymbol{\alpha}}_{(n|n)}$. More specifically in our imposed structure (10), the output estimate $\hat{\boldsymbol{\alpha}}_{(n|n)}$ is obtained from the predicted vector $\hat{\boldsymbol{\alpha}}_{(n|n-1)}$, thanks to the additive correction of the error signal vector $\boldsymbol{v}_{\boldsymbol{\epsilon}(n)}$. And $\boldsymbol{v}_{\boldsymbol{\epsilon}(n)}$ can be regarded as the output of an equivalent "Complex Amplitude Error Detector" (CAED), to be defined in (9) from the new measurement $\mathbf{y}_{\mathbf{p}(n)}$ and the predicted values $\hat{\boldsymbol{\alpha}}_{(n|n-1)}$.

The Time Update Equations are responsible for projecting forward (in time) the current state $\hat{\boldsymbol{\alpha}}_{(n|n)}$ to obtain the *a priori* estimates for the next time step, $\hat{\boldsymbol{\alpha}}_{(n+1|n)}$. More specifically in our imposed structure (12), the prediction $\hat{\boldsymbol{\alpha}}_{(n+1|n)}$ is obtained from the current estimation $\hat{\boldsymbol{\alpha}}_{(n|n)}$ by adding a component proportional to the vector $\boldsymbol{v}_{\mathbf{Lag}(n)}$. And $\boldsymbol{v}_{\mathbf{Lag}(n)}$ defined in (11) is a digital accumulation of the error signal vector $\boldsymbol{v}_{\boldsymbol{\epsilon}(n)}$. Note that at each iteration, we get in fact in $\mu_2 \cdot \boldsymbol{v}_{\mathbf{Lag}}$ an estimate of the *speed evolution* (or slope) of the parameter $\boldsymbol{\alpha}$, useful to predict the parameter evolution for the next iteration.

2) Similitude and difference with a digital PLL structure: From equations (12)&(10), we have $\hat{\boldsymbol{\alpha}}_{(n+1|n)} = \hat{\boldsymbol{\alpha}}_{(n|n-1)} + \mu_1.\boldsymbol{v}_{\boldsymbol{\epsilon}(n)} + \mu_2.\boldsymbol{v}_{\mathbf{Lag}(n)}$. This means that the predicted estimate $\hat{\boldsymbol{\alpha}}_{(n|n-1)}$ can be regarded as the output of a "Complex Amplitude Locked Loop" (CALL). The CALL contains in cascade a "CA Error Detector" (instead of "Phase Error Detector" in a PLL) delivering $\boldsymbol{v}_{\boldsymbol{\epsilon}(n)}$, a standard first-order Lead / Lag loop filter $F_{PLL}(z) = \mu_1 + \frac{\mu_2}{1-z^{-1}}$ delivering $\boldsymbol{v}_{\boldsymbol{c}(n)} = \mu_1.\boldsymbol{v}_{\boldsymbol{\epsilon}(n)} + \mu_2.\boldsymbol{v}_{\mathbf{Lag}(n)}$, and a "Numerically Controlled CA Generator" (instead of a Numerically Controlled Oscillator in a PLL) delivering $\hat{\boldsymbol{\alpha}}_{(n+1|n)} = \hat{\boldsymbol{\alpha}}_{(n|n-1)} + \boldsymbol{v}_{\boldsymbol{c}(n)}$. The figure 1 gives an equivalent scheme of our "Complex Amplitude Tracking Loop" (CATL), which permits to recognize the similitude with a second order digital PLL structure [19]. But our final estimate is not directly the CALL output $\hat{\boldsymbol{\alpha}}_{(n|n-1)}$, but the *a posteriori* estimate (or CATL output) $\hat{\boldsymbol{\alpha}}_{(n|n)}$.

B. Error signal specific to the LS-CATL algorithm

1) Motivation: for one OFDM symbol, the (instantaneous) Squared Distance SD (or squares error) between noisy received pilot subcarriers and corresponding model is defined by

$$S(\hat{\boldsymbol{\alpha}}_{(n)}) = \boldsymbol{d}_{(n)}^H.\boldsymbol{d}_{(n)} \quad (13)$$

where the $N_p \times 1$ error vector is

$$\boldsymbol{d}_{(n)} = \mathbf{y}_{\mathbf{p}(n)} - \boldsymbol{\mathcal{K}}_{(n)}\hat{\boldsymbol{\alpha}}_{(n)} \quad (14)$$

for any estimator $\hat{\boldsymbol{\alpha}}_{(n)}$ of $\boldsymbol{\alpha}_{(n)}$. The LS-estimator of $\boldsymbol{\alpha}_{(n)}$ permits to minimize the SD (13) and can be computed from the observed pilots by

$$\boldsymbol{\alpha}_{\mathbf{LS}(n)} = \mathbf{G}_{(n)}\mathbf{y}_{\mathbf{p}(n)} \quad (15)$$

with

$$\mathbf{G}_{(n)} = \left(\boldsymbol{\mathcal{K}}_{(n)}^H\boldsymbol{\mathcal{K}}_{(n)}\right)^{-1}\boldsymbol{\mathcal{K}}_{(n)}^H \quad (16)$$

where we recall that $\boldsymbol{\mathcal{K}}_{(n)} = \mathrm{diag}\{\mathbf{x}_{\mathbf{p}(n)}\}\mathbf{F}_{\mathbf{p}}$. We see that N_p must fulfill the requirement $N_p \geq L$ in order to allow the pseudo-inverse computation (16) (but $N_p < L$ could be used with a MMSE criterion instead of the

LS criterion). On the other hand, it should be noted that the matrix inversion in (16) has to be done only once when using the same set of pilots from one OFDM symbol to another, or also in the case of 4-QAM symbols. For 4-QAM symbols, the matrix inversion is indeed independent to the index n: $\mathbf{G}_{(n)} = \left(\mathbf{F}_{\mathbf{p}}^H \mathbf{F}_{\mathbf{p}}\right)^{-1} \mathbf{F}_{\mathbf{p}}^H \text{diag}\{\mathbf{x}_{\mathbf{p}(n)}\}^H$. After LS estimation, we obtain from (15)&(16)&(6):

$$\boldsymbol{\alpha}_{\mathbf{LS}(n)} \quad = \quad \boldsymbol{\alpha}_{(n)} + \boldsymbol{\epsilon}_{\mathbf{w}(n)} \tag{17}$$

where $\boldsymbol{\epsilon}_{\mathbf{w}(n)}$ is a zero-mean complex Gaussian noise vector.

2) Error signal: we use the difference between the LS estimator $\boldsymbol{\alpha}_{\mathbf{LS}(n)}$ for the nth OFDM block and the predicted vector parameter for this block, $\hat{\boldsymbol{\alpha}}_{(n|n-1)}$. The error signal vector is then:

$$\boldsymbol{v}_{\boldsymbol{\epsilon}(n)} = \mathbf{G}_{(n)} \mathbf{y}_{\mathbf{p}(n)} - \hat{\boldsymbol{\alpha}}_{(n|n-1)} \tag{18}$$

The specific error signal vector defined in (18) can be expressed in using (15)&(17) versus the prediction error $\boldsymbol{\epsilon}_{Pred(n)} = \boldsymbol{\alpha}_{(n)} - \hat{\boldsymbol{\alpha}}_{(n|n-1)}$ in the most simple linear form:

$$\boldsymbol{v}_{\boldsymbol{\epsilon}(n)} = k_d.\{\boldsymbol{\alpha}_{(n)} - \hat{\boldsymbol{\alpha}}_{(n|n-1)}\} + \boldsymbol{N}_{(n)} \tag{19}$$

The real coefficient k_d is the so called gain of the equivalent CAED, reduced to one here

$$k_d = 1 \tag{20}$$

And $\boldsymbol{N}_{(n)} = [N_{1(n)}, ..., N_{L(n)}]^T$ is a (temporally uncorrelated) zero-mean disturbance due to the additive thermal noise $\mathbf{w}_{\mathbf{p}(n)}$ in input of the CAED, and represents the so-called (input) loop noise ($i.e.$ in *input* of the loop but in *output* of the CAED). With this specific LS-based error signal, we have $\boldsymbol{N}_{(n)} = \boldsymbol{\epsilon}_{\mathbf{w}(n)} = \mathbf{G}_{(n)} \mathbf{w}_{\mathbf{p}(n)}$, with a correlation matrix $E\{\boldsymbol{N}_{(n)}.\boldsymbol{N}_{(n)}^H\} = \sigma^2.\left(\mathbf{F}_{\mathbf{p}}^H \mathbf{F}_{\mathbf{p}}\right)^{-1}$, and a mean variance (per branch or per path, $\sigma_N^2 = \frac{1}{L}.\sum_{l=1}^{L} \sigma_{N_l}^2$):

$$\sigma_N^2 \quad = \quad \frac{\sigma^2}{N_p} \times \lambda_N \tag{21}$$

$$\text{with} \quad \lambda_N \quad = \quad \frac{1}{L}.Tr\{\left(\frac{1}{N_p}.\mathbf{F}_{\mathbf{p}}^H \mathbf{F}_{\mathbf{p}}\right)^{-1}\} \;\geq\; 1 \tag{22}$$

where N_p is the number of pilot sub-carriers. It should be noted that the (input) loop noise variance is minimum ($\sigma_N^2(min) = \frac{\sigma^2}{N_p}$ and $\lambda_N = 1$) if $\boldsymbol{N}_{(n)}$ is uncorrelated from one path to another, $i.e$ when $\mathbf{F}_{\mathbf{p}}^H \mathbf{F}_{\mathbf{p}}$ is a diagonal matrix (this condition depends on the delays distribution).

Special case of first-order loop: if the loop coefficient $\mu_2 = 0$, the on-line estimation algorithm is reduced to an AR1 low-pass filtering of the LS estimator $\boldsymbol{\alpha}_{\mathbf{LS}(n)}$:

$$\hat{\boldsymbol{\alpha}}_{(n|n)} = (1 - \mu_1).\hat{\boldsymbol{\alpha}}_{(n-1|n-1)} + \mu_1.\boldsymbol{\alpha}_{\mathbf{LS}(n)} \tag{23}$$

C. General properties and theoretical MSE analysis

1) Second-order closed-loop transfer function: The estimation error of the tracking algorithm is defined as

$$\boldsymbol{\epsilon}_{(n)} = \boldsymbol{\alpha}_{(n)} - \hat{\boldsymbol{\alpha}}_{(n|n)} \tag{24}$$

We want to get the transfer function between the true vector parameter and the estimate. Combining equations (12) and (10), we have that:

$$\hat{\boldsymbol{\alpha}}_{(n|n)} = \hat{\boldsymbol{\alpha}}_{(n-1|n-1)} + \mu_1.\boldsymbol{v}_{\boldsymbol{\epsilon}(n)} + \mu_2.\boldsymbol{v}_{\mathbf{Lag}(n-1)} \tag{25}$$

By using (11), the Z-domain transform of (25) leads to

$$\hat{\boldsymbol{\alpha}}(z).[1 - z^{-1}] = [\mu_1 + \frac{\mu_2.z^{-1}}{1 - z^{-1}}].\boldsymbol{v}_{\boldsymbol{\epsilon}}(z) \tag{26}$$

Combining the general loop equation (26) with the specific (LS based) error signal (19) rewritten versus the estimation error as

$$\boldsymbol{v}_{\boldsymbol{\epsilon}(n)} = \frac{k_d}{1-k_d\mu_1}.\{\boldsymbol{\alpha}_{(n)} - \hat{\boldsymbol{\alpha}}_{(n|n)}\} + \frac{1}{1-k_d\mu_1}.\boldsymbol{N}_{(n)} \tag{27}$$

leads in the Z-transform domain to

$$\hat{\boldsymbol{\alpha}}(z) = L(z).\boldsymbol{\alpha}(z) + \frac{L(z)}{k_d}.\boldsymbol{N}(z) \tag{28}$$

where $L(z)$ is the transfer function of the CATL defined by

$$L(z) = \frac{\frac{k_d}{1-k_d\mu_1}F(z)}{(1-z^{-1}) \; + \; \frac{k_d}{1-k_d\mu_1}F(z)} \tag{29}$$

with respect to $F(z) = \mu_1 + \frac{\mu_2.z^{-1}}{1-z^{-1}}$. Hence, the CATL transfer function can be written versus the loop coefficients (μ_1, μ_2) as

$$L(z) = \frac{k_d[(z-1)^2.\mu_1 + (z-1).(\mu_1+\mu_2) + \mu_2]}{(z-1)^2 + (z-1).k_d(\mu_1+\mu_2) + k_d\mu_2} \tag{30}$$

or rewritten in a more interpretable form[2] as a function of the couple natural pulsation ω_n (or natural frequency $f_n = \frac{\omega_n}{2\pi}$), and damping factor ζ as

$$L(z) = \frac{2\zeta\omega_n.(1-z^{-1}) + \omega_n^2}{(1-z^{-1})^2 + 2\zeta\omega_n.(1-z^{-1}) + \omega_n^2} \tag{31}$$

$$\text{with:} \quad (\omega_n T)^2 = \frac{k_d\mu_2}{1-k_d\mu_1} \tag{32}$$

$$2\zeta\omega_n T = \frac{(\mu_1-\mu_2)k_d}{1-k_d\mu_1} \tag{33}$$

And from (32) and (33), one given couple (ω_n, ζ) of the second-order low-pass transfer function can be obtained in tuning (μ_1, μ_2) as

$$\mu_1 = \frac{1}{k_d} \cdot \frac{(\omega_n T)^2 + 2\zeta\omega_n T}{1 + (\omega_n T)^2 + 2\zeta\omega_n T} \tag{34}$$

$$\mu_2 = \frac{1}{k_d} \cdot \frac{(\omega_n T)^2}{1 + (\omega_n T)^2 + 2\zeta\omega_n T} \tag{35}$$

The strict stability conditions of $L(z)$ in (30) or (31) will be given in the next subsection for any (μ_1, μ_2). But if we impose the constraint that $0 < \omega_n < +\infty$ and $0 < \zeta < +\infty$ to preserve a physical meaning, we deduce from (34)&(35) that $0 < \mu_2 < \mu_1 < 1/k_d$. We can rewrite $L(z)$ in the frequency-domain, by making $z = e^{pT}$, with $p = j2\pi f$, and f is the frequency variable. Fig. 2 gives the modulus in frequency-domain of the exact function L given in (31). Assuming slow reaction of the loop during one OFDM symbol T ($i.e.$ $f_n.T << 1$), the digital loop transfer function is close (approximation $z^{-1} \approx 1 - p.T$) to the second-order low-pass transfer function usual in analog PLL [27]:

$$L(e^{pT}) \approx \frac{2\zeta\omega_n p + \omega_n^2}{p^2 + 2\zeta\omega_n p + \omega_n^2} \tag{36}$$

Special case of first-order loop: if $\mu_2 = 0$, the transfer function of the system just depends on a cut-off pulsation ω_c (or cut-off frequency $f_c = \frac{\omega_c}{2\pi}$), and is reduced to

$$L(z) = \frac{\omega_c}{(1-z^{-1}) + \omega_c} \tag{37}$$

$$\text{with:} \quad (\omega_c T) = \frac{k_d\mu_1}{1-k_d\mu_1} \tag{38}$$

[2]expression of $L(z)$ is the same than in [18] with $\beta_d = \frac{k_d}{1-k_d.\mu_1}$, but differs to the closed loop transfer function of a 2nd-order digital PLL [26].

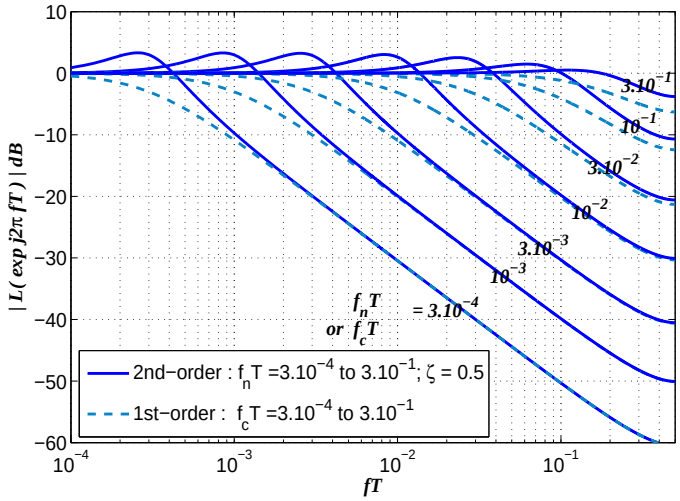

Fig. 2. (exact) Final transfer function $L(z = e^{j2\pi fT})$ versus normalized frequency fT for a second-order loop (continuous line) with various normalized natural frequency $f_nT = 3.10^{-4}$ to $= 3.10^{-1}$ and a damping factor $\zeta = \frac{1}{2}$, and for a first-order loop (dashed line) with various normalized cut-off frequency $f_cT = 3.10^{-4}$ to $= 3.10^{-1}$.

and then approximatively (when $f_c.T << 1$) to an analog first-order low-pass transfer function $L(e^{pT}) \approx \frac{\omega_c}{p+\omega_c}$, as can be seen in Fig. 2. We have from (38) that $\mu_1 = \frac{2\pi f_c T}{1+2\pi f_c T}$.

2) Stability: the condition of stability of the causal rational system $L(z)$ is obtained when all the roots of the denominator polynomial are inside the unit circle. For a 2nd-order denominator polynomial $p(z) = [1 + c_1 z^{-1} + c_2 z^{-2}]$, the stability conditions (obtained by the Schur-Cohn test [28]) are:

$$|c_2| < 1 \quad \text{and} \quad -1 < \frac{c_1}{1+c_2} < 1 \tag{39}$$

with in our case:

$$c_1 = -2 + k_d(\mu_1 + \mu_2) \quad \text{and} \quad c_2 = 1 - k_d\mu_1$$

In summary, $L(z)$ in (30) is stable (for a true second-order system with $\mu_2 \neq 0$) if and only if:

$$0 < k_d\mu_1 < 2 \tag{40}$$

$$0 < k_d\mu_2 < 4 - 2k_d\mu_1 \tag{41}$$

And for the special case of first-order system ($L(z)$ in (37)), only the first equation (40) has to be verified.

3) Mean Squared Error analysis: the estimator is unbiased since the CA estimation error $\boldsymbol{\epsilon}_{(n)}$ defined in (24) is zero-mean (see (28)). Our aim is to compute the estimation error variance $\sigma_\epsilon^2 = \frac{1}{L}.E\{\boldsymbol{\epsilon}_{(n)}^H \boldsymbol{\epsilon}_{(n)}\}$ as

$$\sigma_\epsilon^2 = \sigma_{\epsilon\alpha}^2 + \sigma_{\epsilon N}^2 \tag{42}$$

where $\sigma_{\epsilon\alpha}^2$ is the dynamic error variance, resulting on the variation of the process $\boldsymbol{\alpha}$, and $\sigma_{\epsilon N}^2$ is the static error variance, resulting on the additive thermal noise. According to (28) and (24), the error $\boldsymbol{\epsilon}_{(n)}$ can be expressed in the Z-domain by $\boldsymbol{\epsilon}(z) = (1 - L(z)).\boldsymbol{\alpha}(z) - k_d^{-1}.L(z).\boldsymbol{N}(z)$. Then, the two components of the variance σ_ϵ^2 can be easily expressed. The component $\sigma_{\epsilon\alpha}^2$ results from the high-pass filtering $(1 - L(z))$ of the CAs input $\boldsymbol{\alpha}_{(n)}$:

$$\sigma_{\epsilon\alpha}^2 = \int_{-\frac{1}{2T}}^{+\frac{1}{2T}} \Gamma_\alpha(f).|1 - L(e^{j2\pi fT})|^2 df \tag{43}$$

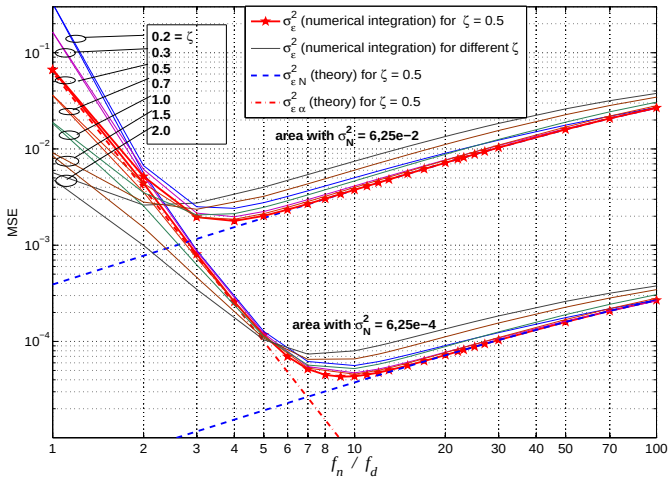

Fig. 3. Network of curves of global $\sigma^2_\epsilon = \sigma^2_{\epsilon\alpha} + \sigma^2_{\epsilon N}$ (continuous line) versus f_n/f_d (for a fixed $f_dT = 1.10^{-3}$) for a second-order loop with various damping factor $\zeta = 0.2, 0.3, 0.5, 0.7, 1, 1.5, 2$ computed numerically from (43) assuming Jakes model (with $\sigma^2_\alpha = 1, L = 6$), and from (44) assuming $k^2_d = 1$ and $\sigma^2_N = 6, 25.10^{-2}$ (top of figure) or $\sigma^2_N = 6, 25.10^{-4}$ (bottom of figure). Theoretical reference (dashed line) given from closed form expressions (45)&(47) for $\sigma^2_{\epsilon N}$, and from (51) for $\sigma^2_{\epsilon\alpha}$

with $\Gamma_\alpha(f) = \frac{1}{L}.\sum_{l=1}^{L}\Gamma_{\alpha_l}$ where Γ_{α_l} is the Power Spectrum Density (PSD) of α_l. And the component $\sigma^2_{\epsilon N}$ results from the low-pass filtering $(-k_d^{-1}.L(z))$ of the input loop noise $\boldsymbol{N}_{(n)}$:

$$\sigma^2_{\epsilon N} = \int_{-\frac{1}{2T}}^{+\frac{1}{2T}} \Gamma_N(f).\frac{1}{k_d^2}.|L(e^{j2\pi fT})|^2 df \tag{44}$$

with $\Gamma_N(f) = \frac{1}{L}.\sum_{l=1}^{L}\Gamma_{N_l}(f)$ where Γ_{N_l} is the PSD of N_l.

If the statistical properties of the stochastic inputs and loop noise are known, the CAs error variance can be computed numerically in evaluating the integrals (43) and (44). The couple (f_n, ζ) has to be properly chosen for a good trade-off between gain tracking ability and loop noise reduction, for a given SNR and f_dT scenario. Fig. 3 gives some numerical integration results for σ^2_ϵ assuming a "Rayleigh-Jakes" model for the CA dynamic, and a (temporally uncorrelated) input loop noise with two different variances σ^2_N. It is shown that fixing $\zeta = \frac{1}{2}$ and varying f_n can be a strategy to obtain the best minimum of σ^2_ϵ. Our objective now is to give some approximate closed form expressions for $\sigma^2_{\epsilon\alpha}$ and $\sigma^2_{\epsilon N}$, especially for $\zeta = \frac{1}{2}$ (or around).

Static error variance $\sigma^2_{\epsilon N}$: since the whiteness of $N_{l(n)}$ can be assumed (with $\Gamma_N(f) = \sigma^2_N T$) for our algorithm, (44) reduces to

$$\sigma^2_{\epsilon N} = \frac{\sigma^2_N}{k_d^2}.B_L \tag{45}$$

where B_L represents the (double-sided normalized) noise equivalent bandwidth of the system, defined by

$$B_L = T \times \int_{-\frac{1}{2T}}^{+\frac{1}{2T}} |L(e^{j2\pi fT})|^2 df \tag{46}$$

An exact analytical expression of B_L can be derived by the method presented by R. Winkelstein in [23] (based on the book of E.I. Jury [29]) for the second-order loop ((30) or (31)), resulting in

$$B_L \;=\; \frac{[8\zeta^2+2](\omega_nT) + 6\zeta(\omega_nT)^2 + (\omega_nT)^3}{8\zeta \;+\; 6\zeta.(\omega_nT) \;+\; (\omega_nT)^3} \tag{47}$$

If $f_n.T << 1$, the approximation leads to the noise equivalent bandwidth of the analog second-order loop given in

(36):

$$B_L \approx 2\pi f_n T.(\zeta + \frac{1}{4\zeta}) \tag{48}$$

And for the first-order loop, the noise equivalent bandwidth is

$$B_{L1} = \frac{2\pi f_c T}{2\pi f_c T + 2} \tag{49}$$

and can be approached when $f_c T << 1$ by $B_{L1} \approx \pi f_c T$.

Dynamic error variance $\sigma^2_{\epsilon\alpha}$: For the "Rayleigh-Jakes" model (5), the Doppler spectrum, $\Gamma_\alpha(f) = \frac{\sigma^2_\alpha / L}{\pi f_d \sqrt{1-(\frac{f}{f_d})^2}}$ for $f \in]-f_d; +f_d[$, has a bounded support. Therefore, a good tracking will require that the natural frequency of the second order loop f_n is greater than f_d. On the other hand, assuming that $f_n << 1/T$, we can deduce that only the Low Frequency (LF) part of the function $|1-L(e^{j2\pi fT})|$ is used in the integral (43). According to (36), the squared modulus of the error transfer function of the second-order loop can be approached in LF (for $f \leq f_n << 1/T$) by $|1-L(e^{j2\pi fT})|^2 \approx \frac{f^4}{f_n^4 + f^2.f_n^2.(4\zeta^2-1)}$. And when moreover $\zeta \approx \frac{1}{2}$, we can use finally the accurate approximation $|1-L(e^{j2\pi fT})| \approx (\frac{f}{f_n})^2$. It results that the CA dynamic error variance $\sigma^2_{\epsilon\alpha}$ in (43) can finally be approached (for $f_d < f_n << 1/T$, and $\zeta \approx \frac{1}{2}$) by

$$\sigma^2_{\epsilon\alpha} \approx \int_{-f_d}^{+f_d} \Gamma_\alpha(f).\left(\frac{f}{f_n}\right)^4 df \tag{50}$$

For the "Rayleigh-Jakes"' model case, a variable change $cos\theta = (f/f_d)$ permits to evaluate (50) analytically as

$$\sigma^2_{\epsilon\alpha}(Jakes) \approx (\frac{3}{8}).\left(\frac{f_d}{f_n}\right)^4.\frac{\sigma^2_\alpha}{L} \tag{51}$$

And for the first-order loop, using from (37) that $|1-L(e^{j2\pi fT})| \approx (\frac{f}{f_c})$ when $f \leq f_d \leq f_c << 1/T$, we have $\sigma^2_{\epsilon\alpha}(Jakes) \approx (\frac{1}{2}).(\frac{f_d}{f_c})^2.\frac{\sigma^2_\alpha}{L}$.

Optimal natural frequency: the dynamic component $\sigma^2_{\epsilon\alpha}$ decreases proportionally to the 4th power of f_n according to (51), whereas the static component $\sigma^2_{\epsilon N}$ increases as a function of f_n, according to (45) and (48). The component $\sigma^2_{\epsilon\alpha}$ (respectively $\sigma^2_{\epsilon N}$) is the dominant part of the global σ^2_ϵ in the low (respectively large) f_n/f_d region, as can be seen in dashed line in the previously mentioned Fig. 3. Now if we fix ζ (around $\frac{1}{2}$), we can calculate the natural frequency f_n that permits (for $f_d < f_n << 1/T$) to minimize the global MSE σ^2_ϵ in (42) as

$$(\frac{f_n}{f_d})(Jakes) = \left(\frac{3}{4}.\frac{1}{\pi}.\frac{1}{(\zeta+\frac{1}{4\zeta})}.\frac{1}{f_d T}.\frac{\sigma^2_\alpha/L}{\sigma^2_N/k_d^2}\right)^{\frac{1}{5}} \tag{52}$$

And the corresponding optimal MSE results in

$$\sigma^2_\epsilon(Jakes) = \lambda \cdot \left(\frac{\sigma^2_\alpha}{L}\right)^{\frac{1}{5}} \cdot \left(\frac{\sigma^2_N}{k_d^2} \cdot f_d T\right)^{4/5} \tag{53}$$

$$\text{with} \quad \lambda = \frac{15}{8} \cdot \left[(\zeta + \frac{1}{4\zeta}) \cdot \frac{4\pi}{3}\right]^{\frac{4}{5}} \tag{54}$$

And for the special case of the first-order loop, the optimal MSE (for $f_d < f_c << 1/T$) is reduced to $\sigma^2_\epsilon(Jakes) = \frac{3}{2}.\left(\frac{\sigma^2_\alpha}{L}\right)^{\frac{1}{3}}.\left(\pi.\frac{\sigma^2_N}{k_d^2}.f_d T\right)^{2/3}$, obtained with

$$(\frac{f_c}{f_d})(Jakes) = \left(\frac{1}{\pi}.\frac{1}{f_d T}.\frac{\sigma^2_\alpha/L}{\sigma^2_N/k_d^2}\right)^{\frac{1}{3}} \tag{55}$$

IV. REFERENCES: KALMAN FILTERS AND BCRB

In the perspective to appreciate the performance of the proposed tracking loop based algorithm, we present in this section three obvious benchmarks that were also investigated to treat our specific problem. We remind the reader that we wish to estimate the CAs $\boldsymbol{\alpha}_{(n)}$ assuming the knowledge of pilots subcarriers $\mathbf{x}_{\mathbf{p}(n)}$ and delays $\boldsymbol{\tau} = [\tau_1, ..., \tau_L]^T$. The estimation is based on the observation model (6) that can be re-formulated as $\mathbf{y}_{\mathbf{p}(n)} = \boldsymbol{\mathcal{K}}\left(\mathbf{x}_{\mathbf{p}(n)}, \boldsymbol{\tau}\right)\boldsymbol{\alpha}_{(n)} + \mathbf{w}_{\mathbf{p}(n)}$. For this specific (parametric channel modeling based) problem, a Kalman filter with an usual first-order Auto-Regressive model (called AR1-Kalman) was first investigated. We developed also a Kalman filter using an optimized second-order model more appropriate under a slow fading channel. In this manuscript, we call this algorithm the (2nd-order) Or2-Kalman filter. Finally, the Bayesian Cramer Rao Bound (BCRB) that provides lower bound on the variance achievable by any unbiased estimator is also given hereafter. Note that other literature channel estimators that operate over the channel transfer function ($i.e$ non-parametric Frequency-Domain estimators) will also be discussed in the simulations section.

A. AR1-Kalman filter and (2nd-order) Or2-Kalman filter

We consider first the Kalman Filter algorithm that can delivers in a sequential manner an estimate of the CAs as proposed in [6] [3]:

$$\hat{\boldsymbol{\alpha}}_{(n|n)} = \text{Kalman}\left(\hat{\boldsymbol{\alpha}}_{(n|n-1)}, \mathbf{y}_{\mathbf{p}(n)}, \mathbf{x}_{\mathbf{p}(n)}, \boldsymbol{\tau}\right)$$

For a so-called Linear Gaussian problem [30], the Kalman filter would give the optimal performance. Exact linear state evolution equation for the Jakes' process CAs are not available. However, we have to give an approximate linear state-space representation of the problem in order to use Kalman filter. In this perspective, the flat fading Rayleigh channel can first commonly be approached by a first-order Auto-Regressive (AR1) model with Gaussian assumption (or Gauss-Markov model) [30], leading to an AR1-Kalman filter [14] [16] [25] [15]. However, in case of slow variations, the CAs variations look like linear during a few symbols, and it could then be more appropriate to consider also second-order model including a (slightly mobile) linear drift δ_l. The general model that we consider to approach the variation of one Jakes'process $\alpha_{l(n)}$ by $\tilde{\alpha}_{l(n)}$ is finally:

$$\tilde{\alpha}_{l(n)} = \gamma.\tilde{\alpha}_{l(n-1)} + \delta_{l(n-1)} \quad (56)$$

$$\delta_{l(n)} = \beta.\delta_{l(n-1)} + u_{l(n)} \quad (57)$$

where γ and β are two positive scalars (lower than 1), $u_{l(n)}$ is zero mean Gaussian complex circular with a variance $\sigma^2_{u_l}$.

First, for the special case of AR1-model (no drift), we have $\beta = 0$, and then $\gamma = R^{(1)}_{\tilde{\alpha}_l}/\sigma^2_{\alpha_l}$ and $\sigma^2_{u_l} = \sigma^2_{\alpha_l}(1-\gamma^2)$. The standard choice for γ becomes $J_0(2\pi f_d T)$ if we impose that the autocorrelation coefficients $R^{(k)}_{\tilde{\alpha}_l}$ of the approximate process perfectly match the Bessel auto-correlation function of the true Jakes process in (5) for lag $k \in \{-1; 0; 1\}$ (or for $k \in \{-p;\ ...; 0;\ ...; p\}$ for a model with order p). But we can use a more general choice as in [13], with:

$$\gamma = \frac{J_0(2\pi f_d T)}{1+\epsilon} \qquad \text{(AR1-Kalman)}$$

where ϵ is a possible very small positive amount ($<< 1$). This slight change can create a more *regular* process that in some sense closely approximates the original process. The specific equations of the AR1-Kalman filter applied to our model can be found in [18].

Secondly, for the second-order model, the coefficient β is chosen close to one (but lower) to introduce a drift with time. And the parameters of the model have to be calibrated such that the slope (or drift) of the CA variation, $\delta_{l(n)}$, changes slowly with time n, according to the actual value of $f_d T$. From the relationship between $R^{(2)}_{\tilde{\alpha}_l}$ and $R^{(1)}_{\tilde{\alpha}_l}$ obtained from (56)&(57), we find that the coefficient γ can be computed, for a given β, by

$$\gamma = \frac{R^{(2)}_{\tilde{\alpha}_l} - \beta R^{(1)}_{\tilde{\alpha}_l}}{R^{(1)}_{\tilde{\alpha}_l} - \beta.\sigma^2_{\alpha_l}} \qquad \text{(Or2-Kalman)}$$

[3] considering in [6] the Kalman-(forward-only)-initial estimation based on pilots. More precisely [6] is the Time-Domain channel estimator that estimates the discrete-time impulse response including both physical channel (CAs at known positions $\boldsymbol{\tau}$) and receive filter.

where we can still impose $R^{(1)}_{\tilde{\alpha}_l} = \frac{\sigma^2_{\alpha_l}}{(1+\epsilon)} J_0(2\pi f_d.T)$, and now $R^{(2)}_{\tilde{\alpha}_l} = \sigma^2_{\alpha_l} J_0(2\pi f_d.2T)$ for lag $k=2$. The state-noise variance is $\sigma^2_{u_l} = \sigma^2_{\delta_l}(1-\beta^2)$, where $\sigma^2_{\delta_l} = \sigma^2_{\alpha_l}(1+\gamma^2) - 2\gamma.R^{(1)}_{\tilde{\alpha}_l}$ is the variance of the drift δ_l. The 2nd-order model of the CAs evolution can be re-formulated in a state-space model. The state vector to be considered includes the CA and the drift for each path, $\boldsymbol{a}_{(n)} = [\boldsymbol{a}^T_{1(n)}, \boldsymbol{a}^T_{2(n)}, ..., \boldsymbol{a}^T_{L(n)}]^T$, where $\boldsymbol{a}_{l(n)} = [\tilde{\alpha}_{l(n)}, \delta_{l(n)}]^T$. The state evolution matrix is $\mathbf{M} = \text{blkdiag}\{\mathbf{M}_1, ..., \mathbf{M}_L\}$, where $\mathbf{M}_l = \begin{bmatrix} \gamma & 1 \\ 0 & \beta \end{bmatrix}$ for $l = 1...L$, and the state-noise vector is $\mathbf{u}_{(n)} = [0, u_{1(n)}, ..., 0, u_{L(n)}]^T$. The observation matrix with size $N_p \times 2L$ is $\mathbf{S}_{(n)} = \boldsymbol{\mathcal{K}}_{(n)}\mathbf{Z}$, where $\mathbf{Z} = [\mathbf{1}_L, \mathbf{0}_L, ..., \mathbf{1}_L, \mathbf{0}_L]$, with $\mathbf{1}_L$ being a column vector with L ones, and $\mathbf{0}_L$ with L zeros. From this we obtain the state evolution (56)&(57) and the observation equation (6) in a state-space formulation as

$$\begin{aligned} \boldsymbol{a}_{(n)} &= \mathbf{M}\boldsymbol{a}_{(n-1)} + \mathbf{u}_{(n)} \quad (58) \\ \mathbf{y}_{\mathbf{p}(n)} &= \mathbf{S}_{(n)}\boldsymbol{a}_{(n)} + \mathbf{w}_{\mathbf{p}(n)} \quad (59) \end{aligned}$$

The two stages of the so called *Or2-Kalman* filter are:

Time Update Equations:

$$\begin{aligned} \hat{\boldsymbol{a}}_{(n|n-1)} &= \mathbf{M}\hat{\boldsymbol{a}}_{(n-1|n-1)} \\ \mathbf{P}_{(n|n-1)} &= \mathbf{M}\mathbf{P}_{(n-1|n-1)}\mathbf{M}^H + \mathbf{U} \quad (60) \end{aligned}$$

Measurement Update Equations:

$$\begin{aligned} \mathbf{K}_{(n)} &= \mathbf{P}_{(n|n-1)}\mathbf{S}^H_{(n)}\left(\mathbf{S}_{(n)}\mathbf{P}_{(n|n-1)}\mathbf{S}^H_{(n)} + \sigma^2\mathbf{I}_{N_p}\right)^{-1} \\ \hat{\boldsymbol{a}}_{(n|n)} &= \hat{\boldsymbol{a}}_{(n|n-1)} + \mathbf{K}_{(n)}\left(\mathbf{y}_{p(n)} - \mathbf{S}_{(n)}\hat{\boldsymbol{a}}_{(n|n-1)}\right) \\ \mathbf{P}_{(n|n)} &= \mathbf{P}_{(n|n-1)} - \mathbf{K}_{(n)}\mathbf{S}_{(n)}\mathbf{P}_{(n|n-1)} \quad (61) \end{aligned}$$

where $\mathbf{K}_{(n)}$ is the Kalman gain matrix and $\mathbf{U} = \text{diag}\left\{0, \sigma^2_{u_1}, ..., 0, \sigma^2_{u_L}\right\}$.

B. Bayesian Cramer Rao Bound (BCRB)

The on-line BCRB for the estimation of $\boldsymbol{\alpha}_{(n)}$ from actual and previous observations over a multi-path Rayleigh fading channel and OFDM modulation has been derived in [4] for the Data-Aided or Non Data-Aided contexts. The adaptation of [4] for our pilot-based observation model $[\mathbf{y}_{\mathbf{p}(1)}, ..., \mathbf{y}_{\mathbf{p}(n)}]$ implies that for any unbiased estimator $\hat{\boldsymbol{\alpha}}_{(n)}$ of $\boldsymbol{\alpha}_{(n)}$:

$$\frac{1}{L}.\text{E}\{(\boldsymbol{\alpha}_{(n)} - \hat{\boldsymbol{\alpha}}_{(n)})^H.(\boldsymbol{\alpha}_{(n)} - \hat{\boldsymbol{\alpha}}_{(n)})\} \geq \text{BCRB}_{(n)}$$

where the on-line BCRB reduces to

$$\begin{aligned} \text{BCRB}_{(n)} &= \frac{1}{L}.\sum_{i=(n-1)L+1}^{nL} [\mathbf{BCRB}(n)]_{ii} \quad (62) \\ \text{with } \mathbf{BCRB}(n) &= \left(\text{blkdiag}\left\{\mathbf{J}_m, \mathbf{J}_m, ..., \mathbf{J}_m\right\} + \mathbf{R}^{-1}_{\boldsymbol{\alpha}}\right)^{-1} \end{aligned}$$

where $\mathbf{J}_m = \frac{1}{\sigma^2}\mathbf{F}^H\mathbf{F}$ is a $L \times L$ matrix, and the covariance matrix $\mathbf{R}_{\boldsymbol{\alpha}}$ of size $nL \times nL$ is defined by the elements:

$$[\mathbf{R}_{\boldsymbol{\alpha}}]_{i(l,p),i(l',p')} = \begin{cases} \text{R}^{(p-p')}_{\alpha_l} & \text{for } l'=l \in[1,L] \quad p,p'\in[0,n-1] \\ 0 & \text{for } l'\neq l \quad '' \end{cases}$$

with $i(l,p) = 1 + (l-1) + pL$ and $\text{R}^{(p)}_{\alpha_l}$ defined in (5). In the simulation results, we will plot $\text{BCRB} = \text{BCRB}_{(\infty)}$ as reference.

V. Simulations

In this section, the performance of the LS-CATL algorithm is evaluated, first confronted with theoretical analysis and section IV references (AR1-Kalman, Or2-Kalman, BCRB), and next with literature algorithms. By default, we

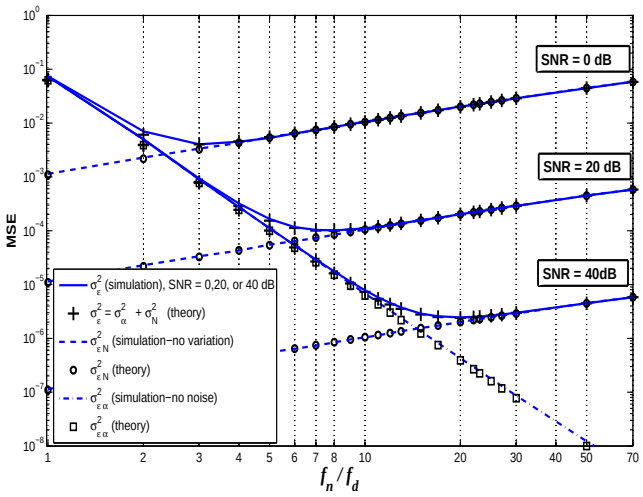

Fig. 4. Comparison between simulated and theoretical MSE vs f_nT for $f_dT = 10^{-3}$, $\zeta = 0.5$, SNR = 0, 20, or 40 dB, $N_p = 16$ for proposed 2nd-order LS-CATL algorithm. Theoretical values are given from (45)&(47) for $\sigma^2_{\epsilon N}$, and from (51) for $\sigma^2_{\epsilon\alpha}$.

used a 4QAM-OFDM system (but other sizes of QAM modulation are also considered), $N = 128$ subcarriers, $N_g = \frac{N}{8} = 16$ samples for the cyclic prefix, and $\frac{1}{T_s} = 2MHz$. The number of pilot subcarriers was $N_p = 6, 8, 16,$ or 32, corresponding to a distance between pilot subcarriers $L_f = 22, 16, 8,$ or 4 respectively. We used the same set of pilots for each OFDM symbols. The channel model is a Jakes'spectrum Rayleigh channel model with $L = 6$ paths and maximum delay $\tau_{max} = 10$ (expressed as a fraction of T_s), and corresponds to the GSM model [1] [11] recalled in table I. The performance is evaluated under a slowly time-varying channel with $f_dT \leq 10^{-2}$ (corresponding to a vehicle speed $V_m \leq 140\ km/h$ for $f_c = 1GHz$), with a default value $f_dT = 10^{-3}$.

$Path\ number\ l$	1	2	3	4	5	6
$\sigma^2_{\alpha l}/\sigma^2_\alpha\ (dB)$	-3	0	-2	-6	-8	-10
τ_l	0	1	2	3	4	10

TABLE I
AVERAGE POWERS AND (NORMALIZED) DELAYS OF THE CHANNEL

A. Confrontation with theory and with section IV references

1) Confrontation with theoretical analysis versus f_nT: Fig. 4 gives comparison between simulated and theoretical error variances versus f_nT for $f_dT = 10^{-3}$, and SNR = 0, 20, or 40 dB for proposed 2nd-order (LS-CATL) algorithm, with $N_p = 16$ pilot subcarriers. The simulated dynamic error variance $\sigma^2_{\epsilon\alpha}$ was obtained in forcing the noise $\mathbf{w_p}(n)$ to zero, whereas the simulated static error variance $\sigma^2_{\epsilon N}$ was obtained in maintaining the CAs of the paths to constant values equal to their standard deviations σ_l. First of all, we can observe that all the theoretical curves are very close to the simulated ones. Therefore, the abscissa of the minimum of the simulated MSE σ^2_ϵ matches also very well with the (theoretical closed form (52)) optimal natural frequency (such that $f_n/f_d\ (Jakes)$ = 3, 7.4 and 18.7 respectively for SNR = 0, 20, and 40 dB, with $N_p = 16$). It is interesting to note that there is a large range around the optimal natural frequency for which the MSE remains very close to the minimum value (for any SNR). Hence, the tuning of natural frequency of the loop coefficients does not need to be very accurate.

2) Performance comparison: In the following, we use the parameters that yield around the best possible performance, for the various algorithms. For the proposed LS-CATL algorithm, Tables II(a) and II(b) give the loop parameters used (theoretical values from (52) are also given) for $f_dT = 10^{-3}$ and $f_dT = 10^{-2}$ respectively, with $N_p = 16$ pilot subcarriers. According to this tables given as examples, but also more generally, we have observed that for the 2nd-order proposed algorithm, the optimal f_n were very close to the theoretical values for $f_dT \leq 10^{-3}$, and still are close up to $f_dT = 10^{-2}$ (so for our slow-fading assumption). And for the 1st-order version of the algorithm, closed form expressions and observed values of the optimal cut-off frequency f_c match well only for $f_dT \leq 10^{-3}$ and low SNR. For the AR1-Kalman and the Or2-Kalman filters, the parameters (γ, β)

used and the corresponding ϵ (that yield around the best possible performance) are given in table III (performance with $\epsilon = 0$ for the AR1-Kalman will also be plotted in thin dotted lines, as in [18]).

$SNR\ (dB)$	0	5	10	15	20	25	30	35	40
f_n/f_d	3	4	5	6	8	10	12	15	20
(theory (52))	3	3.7	4.7	5.9	7.4	9.4	11.8	14.8	18.7
f_c/f_d	7	10	15	22	34	50	80	130	200
(theory (55))	6.7	9.9	14.5	21.2	31.2	45.7	67.1	98.5	145

(a) for $f_dT = 10^{-3}$

$SNR\ (dB)$	0	5	10	15	20	25	30	35	40
f_n/f_d	2	2.5	3	4	5	6	8	12	15
(theory (52))	1.9	2.4	3	3.7	4.7	5.9	7.4	9.4	11.8
f_c/f_d	3	5	7	10	24	30	50	90	400

(b) for $f_dT = 10^{-2}$

TABLE II
LOOP PARAMETERS FOR THE 2ND-ORDER LOOP (f_n/f_d) AND THE 1ST-ORDER LOOP (f_c/f_d), FOR $N_p = 16$ AND $f_dT = 10^{-3}$, 10^{-2}

	$f_dT = 10^{-3}$		$f_dT = 10^{-2}$	
	AR1-Kalman	Or2-Kalman	AR1-Kalman	Or2-Kalman
β	0	0.9992	0	0.98
γ	0.9996	0.9978	0.9921	0.9975
ϵ	4.10^{-4}	9.10^{-6}	8.10^{-3}	8.10^{-4}

TABLE III
PARAMETERS (β, γ) USED (AND CORRESPONDING ϵ) FOR THE AR1-KALMAN AND OR2-KALMAN, FOR $f_dT = 10^{-3}, 10^{-2}$

Fig. 5(a) and Fig. 5(b) show the evolution of MSE versus SNR, respectively for $f_dT = 10^{-3}$ and $f_dT = 10^{-2}$. First of all, the MSE of the 2nd-order (respectively 1st-order) proposed LS-CATL algorithm is very close to the one obtained by the Or2-Kalman (respectively AR1-Kalman) algorithm. It is gratifying to observe that the reduced complexity algorithm exhibits quasi the same asymptotic variance than the reference Kalman algorithm, for a same model order. It was our desired objective, motivated by some interesting known results for the phase estimation problem based on PLL. Indeed, some others have previously proved that the PLL can be interpreted as a form of Kalman filter [20] [31], with equivalent MSE asymptotic performance (in tracking mode[4]) if a satisfactory dynamic model is available [21]. Secondly, we observe on the one hand that the performance of the AR1-Kalman algorithm, despite its complexity, does not reach the BRCB in case of slow channel variation (more notable for $f_dT = 10^{-3}$ than for $f_dT = 10^{-2}$). On the other hand, with a second-order loop (or an Or2-Kalman filter), the MSE becomes closer to the BCRB. This point reveals the advantage of a second-order loop versus a first-order loop ($i.e.\ \mu_2 = 0$) in slow fading scenario. It emphasizes the benefit of the integration, that is inherent to the second-order loop, but not included in the AR1-Kalman algorithm. It allows a higher decrease of the MSE that is proportional to the $(\frac{4}{5})$ power of the SNR, in full agreement with the closed form expression (53), also validated on these figures (still more exactly for $f_dT = 10^{-3}$ than for $f_dT = 10^{-2}$).

Fig. 6 (up) shows again the MSE performance improvement achieved by the 2nd-order against 1st order loop, for a given number of pilot subcarriers N_p from 6 (minimum value permitted with $L = 6$ paths for the LS-CATL algorithm) to 32, or for a given normalized Doppler frequency f_dT from 10^{-5} to 10^{-2}. This performance improvement is seen more important for smallest f_dT (whereas for high speed channel such that $f_dT \geq 10^{-1}$, the AR1-Kalman would closely approach the BCRB according to [12], Fig. 3). In agreement with the theoretical analysis (53), the MSE increases proportionally to the $(\frac{4}{5})$ power of f_dT for the 2nd-order loop for all the range of $f_dT \leq 10^{-2}$ (versus a power $(\frac{2}{3})$ for the 1st-order loop, verified only for $f_dT \leq 10^{-3}$). On the other hand, it is

[4]Kalman filter equations can be regarded as equivalent loop equations as soon as the Kalman gain converges and becomes time invariant.

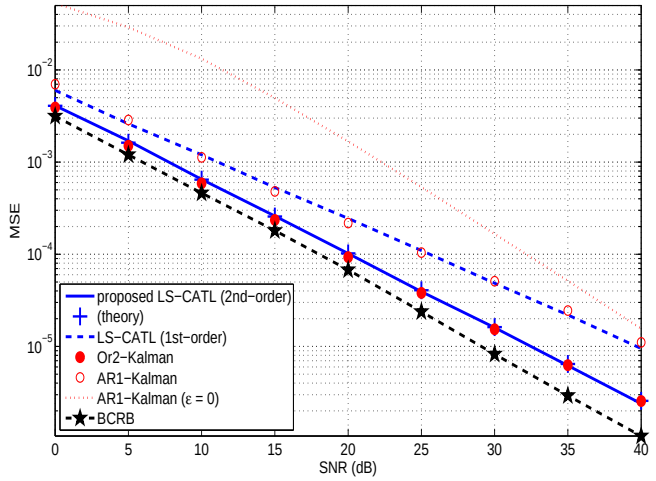

(a) $f_dT = 10^{-3}$

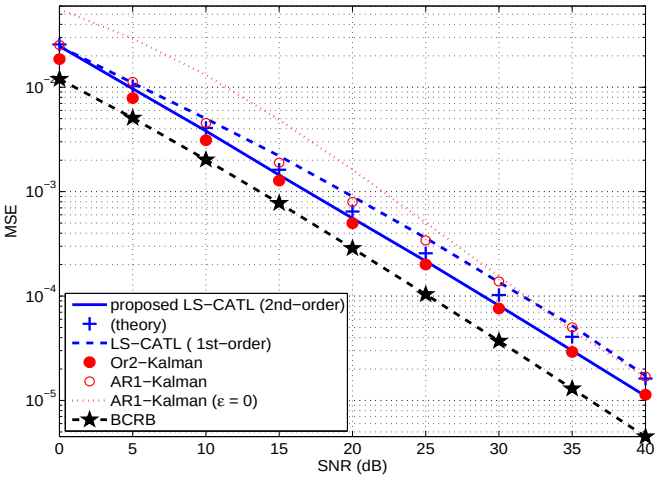

(b) $f_dT = 10^{-2}$

Fig. 5. MSE vs SNR for $f_dT = 10^{-3}$ (a) and $f_dT = 10^{-2}$ (b), with $N_p = 16$

normal to observe that when the number of pilots is increased, the MSE decreases. Fig. 6 (down) informs on the value of the optimal natural frequency f_n normalized by f_d, for a given N_p or a given f_dT. Note that the optimal f_n/f_d (52) (and also the optimal MSE (53)) depends on the input loop noise variance σ_N^2 (21), which is inversely proportional to N_p but also proportional to a factor $\lambda_N \geq 1$. For the given channel, this factor still depends on N_p (actually $\lambda_N = 13.7, 3.7, 2.8, 2.7$ respectively for $N_p = 6, 8, 16, 32$), and is greater than one because the $N_p \times N_p$ matrix $\mathbf{F_p}^H\mathbf{F_p}$ is not diagonal.

Fig. 7 shows the evolution of the Bit Error Rate (BER) in the case of 4-QAM, 16-QAM and 64-QAM modulations for the previous channel estimators completed by a Zero-Forcing (ZF) frequency-domain equalizer (the channel frequency response is previously estimated from the CA estimates $\hat{\boldsymbol{\alpha}}_{(n)}$ by $\hat{\boldsymbol{\mathcal{H}}}_{(n)} = \mathbf{F}\hat{\boldsymbol{\alpha}}_{(n)}$, before equalization). For the sake of comparison, we also plotted the BER obtained with perfect knowledge of the channel. The BER results agree with the previous MSE results, but with lower difference between the curves due to decision process. Hence, the performance with our 2nd-order LS-CATL algorithm is now the same in terms of BER than with the Or2-Kalman algorithm, and is slightly better (for low SNR regions) than with the AR1-Kalman (and then the 1st-order LS-CATL). The BER performances are close to that found with a ZF equalizer using perfect channel knowledge. When increasing the size of the modulation, the BER curves are obviously shifted toward highest SNR. And for a given BER, the gap between 1st-order and 2nd-order algorithms (in terms of required SNR) is also slightly increased with the modulation size.

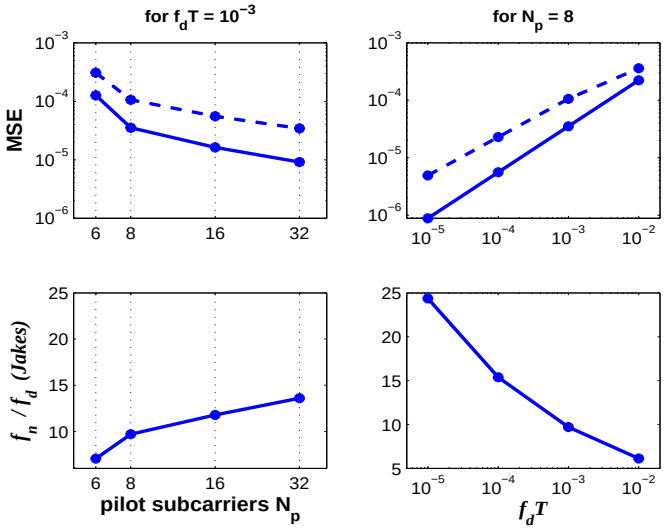

Fig. 6. Evolution of the MSE (up) and of the corresponding optimal f_n/f_d (down) for the proposed CATL algorithm (2nd-order in continuous line, 1st-order in dashed line) for $SNR = 30$dB versus the number of pilot subcarriers (left, for a fixed $f_dT = 10^{-3}$) and versus f_dT (right, for a fixed $N_p = 8$)

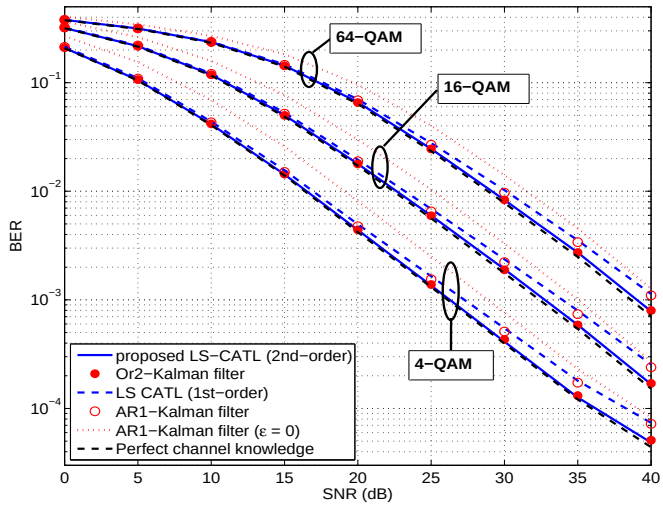

Fig. 7. BER comparison for the case of 4-QAM, 16-QAM or 64-QAM modulation for $f_dT = 10^{-3}$ and $N_p = 8$

B. Bench marking

Now, we bench mark the BER performance of the proposed LS-CATL algorithm by other estimators that have been suggested in literature. Specifically, we consider Frequency Domain (FD) channel estimator described in introduction section that estimates the frequency response of the channel $\boldsymbol{\mathcal{H}}_{(n)}$ for the N subcarriers assuming the knowledge of N_p pilots subcarriers $\mathbf{x}_{\mathbf{p}(n)}$. The estimation is based on the observation model (equivalent to (6)): $\mathbf{y}_{\mathbf{p}(n)} = \text{diag}\{\mathbf{x}_{\mathbf{p}(n)}\}\boldsymbol{\mathcal{H}}_{\mathbf{p}(n)} + \mathbf{w}_{\mathbf{p}(n)}$, where $\boldsymbol{\mathcal{H}}_{\mathbf{p}(n)} = \mathbf{F}_{\mathbf{p}}\boldsymbol{\alpha}_{(n)}$. The algorithms are summarized as follows:

- "conventional" LS(FD)-LPI [2]: employs LS criterion to estimate the channel at pilot frequencies: $\hat{\boldsymbol{\mathcal{H}}}_{\mathbf{p}(n)} = \text{diag}\{\mathbf{x}_{\mathbf{p}(n)}\}^{-1}\mathbf{y}_{\mathbf{p}(n)}$ and then makes LPI interpolation: $\hat{\boldsymbol{\mathcal{H}}}_{(n)} = \mathbf{LPI}\{\hat{\boldsymbol{\mathcal{H}}}_{\mathbf{p}(n)}\}$.
- Kalman(FD)-LPI [5][5]: employs (per-subchannel) AR-Kalman filter to estimate the channel at pilot frequencies: $\hat{\boldsymbol{\mathcal{H}}}_{\mathbf{p}(n|n)} = \text{Kalman}\left(\hat{\boldsymbol{\mathcal{H}}}_{\mathbf{p}(n|n-1)}, \mathbf{y}_{\mathbf{p}(n)}, \mathbf{x}_{\mathbf{p}(n)}\right)$ and then makes LPI Interpolation: $\hat{\boldsymbol{\mathcal{H}}}_{(n)} = \mathbf{LPI}\{\hat{\boldsymbol{\mathcal{H}}}_{\mathbf{p}(n|n)}\}$.

Moreover, if the knowledge of delays $\boldsymbol{\tau}$ is available, the previous (blind) LPI interpolation can be replaced by a Delays-Based-Interpolation (DBI), $\hat{\boldsymbol{\mathcal{H}}}_{(n)} = \mathbf{DBI}\{\hat{\boldsymbol{\mathcal{H}}}_{\mathbf{p}(n)}, \boldsymbol{\tau}\}$, consisting in: $\hat{\boldsymbol{\mathcal{H}}}_{(n)} = \left(\mathbf{F}\left(\mathbf{F}_{\mathbf{p}}^H\mathbf{F}_{\mathbf{p}}\right)^{-1}\mathbf{F}_{\mathbf{p}}^H\right)\hat{\boldsymbol{\mathcal{H}}}_{\mathbf{p}(n)}$. This

[5]the per-subchannel Kalman filter has been adapted to our pilot scheme since [5] considered a full block of pilots

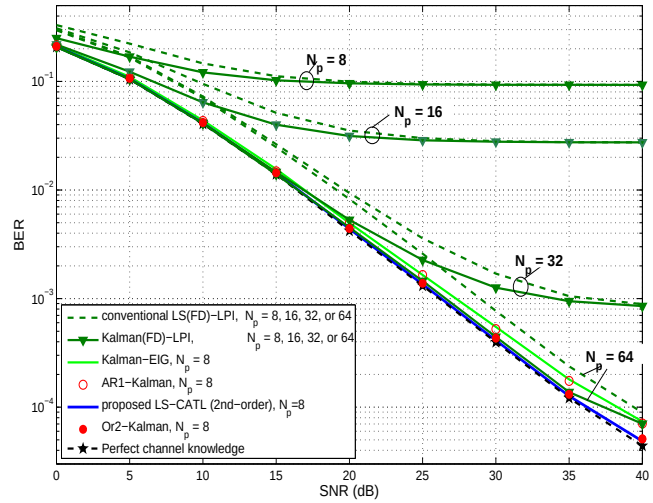

(a) $f_dT = 10^{-3}$

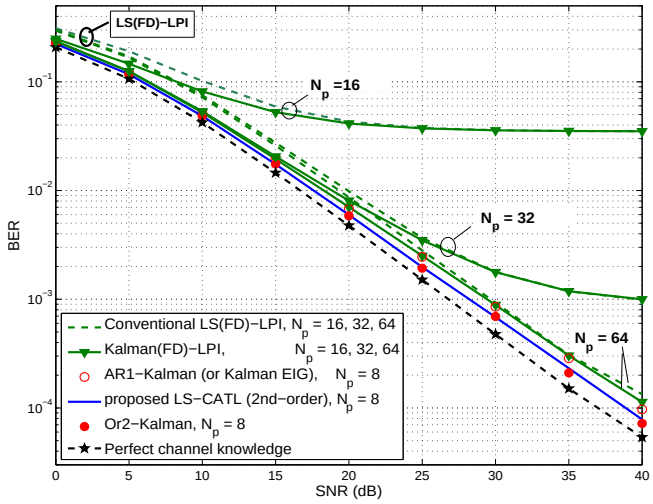

(b) $f_dT = 10^{-2}$

Fig. 8. BER comparison with various literature methods using equal or greater number of pilot sub-carriers N_p than the proposed method, for $f_dT = 10^{-3}$ (a) and for $f_dT = 10^{-2}$ (b)

procedure leads to the two new versions of the previous algorithms:

- LS(FD)-DBI
- Kalman(FD)-DBI

A last algorithm that requires also the availability of the power-delay profile (in the version we have implemented) is based on an "eigenvalues interpolation":

- Kalman-EIG [7] [6]: in this parameter reduction approach, the channel frequency response (N subcarriers) is computed by $\hat{\boldsymbol{\mathcal{H}}}_{(n|n)} = \mathbf{V}\hat{\boldsymbol{e}}_{(n|n)}$, where $\mathbf{V}$ contains the $N_e << N$ dominant eigenvectors of the FD channel correlation matrix $\mathbf{R}_{\boldsymbol{\mathcal{H}}}(\boldsymbol{\tau}) = \mathbf{F}\text{diag}\left\{\sigma^2_{\alpha_1}, ..., \sigma^2_{\alpha_L}\right\}\mathbf{F}^H$ assumed here perfectly known. The subspace coefficients are previously estimated by an AR1-Kalman filter: $\hat{\boldsymbol{e}}_{(n|n)} = \text{Kalman}\left(\hat{\boldsymbol{e}}_{(n|n-1)}, \mathbf{y}_{\mathbf{p}(n)}, \mathbf{x}_{\mathbf{p}(n)}\right)$.

Fig. 8(a) shows for $f_dT = 10^{-3}$ (and Fig. 8(b) for $f_dT = 10^{-2}$) the BER performance, using a ZF equalizer and a 4-QAM modulation, of the 2nd-order proposed LS-CATL algorithm (and previous AR1-Kalman and Or2-Kalman references) and three aforementioned literature methods (conventional LS(FD)-LPI, Kalman(FD)-LPI, Kalman-EIG). It is first of all highly noteworthy that the "first category" of algorithms (proposed algorithm, Or2-Kalman, AR1-Kalman and Kalman-EIG) greatly outperforms the conventional LS(FD)-LPI method even if the latter uses

[6] corresponds to the initial (pilot-based) channel estimator in [7]

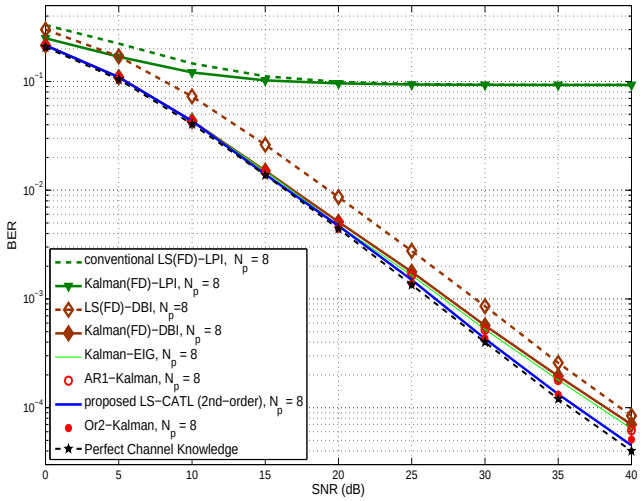

Fig. 9. BER comparison vs SNR for $f_dT = 10^{-3}$ with various methods, all assuming knowledge of delays-related information (with $N_p = 8$)

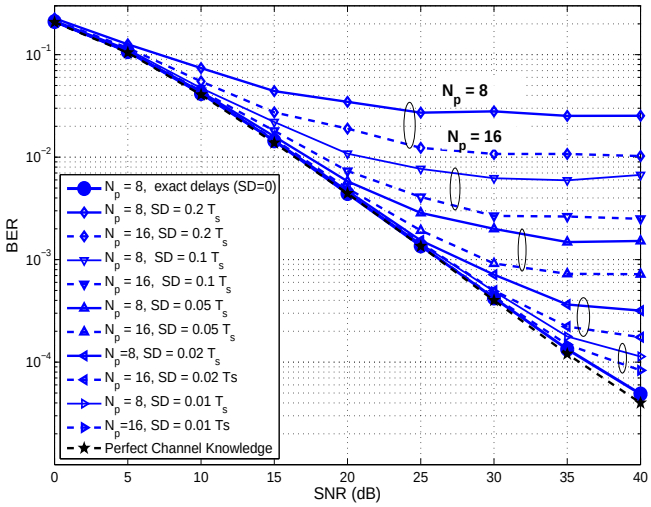

Fig. 10. BER of the proposed 2nd-order LS-CATL algorithm for the case of imperfect knowledge of the delays for $f_dT = 10^{-3}$ (with $N_p = 8$ or 16)

a greater number[7] of pilot subcarriers ($N_p = 64$ versus only $N_p = 8$). These results permit to measure the gain when exploiting time domain correlation, frequency domain correlation, as well as knowledge of the delays-related information (first category) versus only frequency correlation (conventional). When the conventional symbol by symbol LS(FD)-LPI method is extended into Kalman(FD)-LPI algorithm to improve the estimation of the channel at pilot frequency positions (before performing the LPI interpolation in frequency-domain), we can measure the increase in performance due only to the incorporation of time correlation over several symbols. The benefit of the time-filtering is mainly observed in low SNR region, and more notable for the lower f_dT because of a strongest channel time-correlation. But the resulting performance remains still far from that of the "first category" of algorithms, unless if $N_p = 64$ pilot subcarriers are used ($i.e.$ a distance $L_f = 2$ between two pilot subcarriers). Hence, the availability or the non-availability of the delay-related information is an assumption that influences strongly the channel estimator performance, and will be discussed later. Considering now the Kalman-EIG algorithm, the BER performance is close to that found with perfect channel knowledge, and is the same than that obtained with the AR1-Kalman algorithm (and then the 1st-order LS-CATL algorithm). It is quite understandable since

[7]for the LPI interpolation, the number of pilot subcarriers must actually fulfill $N_p \geq 10$ for our considered scenario if we impose to satisfy the sampling theorem (with then a sampling rate in frequency domain L_f such that [8]: $\frac{N}{L_f} \geq \frac{\tau_{max}}{T_s} = 10$).

both algorithms use Kalman filter based on the same AR1 state-space model (we take the same value for ϵ) with 6 dominant eigenvalues tracked in the parameter reduction approach, against L=6 paths CAs tracked in the AR1-Kalman, and the tracking is performed from a same number of pilot subcarriers $N_p = 8$.

Fig. 9 compares the BER performance of the previous algorithms with that achieved when using LS(FD)-DBI and Kalman(FD)-DBI algorithms, for a same number of pilot sub-carriers fixed to $N_p = 8$. These two algorithms are respectively the extension of conventional LS(FD)-LPI and Kalman(FD)-LPI by replacing the (blind) interpolation LPI by the interpolation based on the knowledge of the delays. It permits now to compare algorithms with equivalent assumptions, contrary to the case of the previous figures. The great performance gap between -LPI and -DPI versions allows to measure the strong potential improvement in the channel estimation if delay-related information is available. The improvement due to the a priori knowledge of the delays is predominant in large SNR region. On the other hand, comparison between LS(FD)- and Kalman(FD)- versions permits to measure again the gain in performance when exploiting time correlation, interesting for low SNR region. It is finally not surprising to observe that the Kalman(FD)-DBI algorithm and the AR1-Kalman algorithm exhibit the same performance (both are based on the same scheme: "FD-pilots based estimation $\Rightarrow$ CAs $\Rightarrow$ FD-all subcarriers", but with a time-integration by the Kalman filter performed in first or second position). The availability of the delay related information permits a strong improvement compared to conventional methods, but the price to be paid is the requirement of an accurate delays acquisition procedure.

C. Robustness of the LS-CATL algorithm to an imperfect delay knowledge

Fig. 10 measures the effect of an imperfect delay knowledge on the BER performance of our second-order proposed algorithm. SD denotes the standard deviation of the time delay errors (modeled as zero mean Gaussian variables). As expected (common drawback to any parametric channel estimator), the algorithm performance decreases with respect to the delay error. However, the algorithm is not very sensitive to a delay error $SD < 0.05T_s$ in low SNR, and $SD < 0.02T_s$ in high SNR, despite a weak number of pilot subcarriers $N_p = 8$. And when increasing the number of pilot subcarriers to $N_p = 16$, sensibility to delay error is weak for $SD < 0.1T_s$ in low SNR, and for $SD < 0.05T_s$ in high SNR. These required performance for the delays acquisition can well be obtained when using high resolution algorithms [8], thanks to the quasi invariance of the delays (with respect to the scale of the sampling time T_s) during a large number of OFDM symbols, especially in the slow fading case (see also performance in [11] Fig. 10, or in [12] obtained by the ESPRIT method [8] for the same channel and pilot scheme than here but a more unfavorable scenario due to higher mobility $f_dT = 0.1$, or 0.3). In conclusion, when combined with an accurate delay acquisition procedure, the proposed algorithm still provides interesting increase in performance compared to conventional methods based on LPI.

VI. CONCLUSION

Channel paths complex amplitude estimator over slow-fading channels has been proposed and analyzed. It can be directly useful for (Data Aided or Data Directed) mono-carrier systems over flat fading channel. Applied to OFDM systems (with pilot subcarriers), it belongs to the class of algorithms that performs the tracking of the CAs of a multi-path channel, from the delays related information (assuming therefore a previous delays acquisition procedure). The proposed algorithm is based on a second-order recursive loop, that integrates an error signal built from the (pilot based) LS estimates of the CAs. It permits to exploit the time-domain correlation of the channel in a simple manner, compared to Kalman based methods that require matrix inversion (to compute the Kalman gain matrix) at each iteration. Simulation results show that the MSE performance of the 2nd-order proposed algorithm is very close to that of a Kalman estimator based on a 2nd-oder approximation of the true channel. Moreover, our 2nd-order algorithm outperforms the more complex Kalman estimator when the later is based only on a first-order Auto-Regressive approximation, which emphasizes the interest for the 2nd-order versus 1st-order methods in case of slow fading variation ($f_dT \leq 10^{-2}$). We have given closed form expressions of the optimal natural frequency of the loop, and corresponding minimum MSE (assuming Rayleigh-Jakes channel). It is demonstrated that the MSE of our 2nd-order algorithm decreases proportionally to the $(\frac{4}{5})$ power of the SNR, and increases proportionally to the $(\frac{4}{5})$ power of the normalized Doppler frequency f_dT. Finally, BER comparison through simulation has shown that the proposed algorithm outperforms the basic conventional method based on LPI interpolation in the frequency domain.

Moreover, simulations have also shown that the proposed algorithm is rather robust to a reasonable mismatch in the knowledge of the delays.

REFERENCES

[1] Y. Zhao and A. Huang, "A novel Channel estimation method for OFDM Mobile Communications Systems based on pilot signals and transform domain processing" in *Proc. IEEE 47th Vehicular Techno. Conf.*, Phonix, USA, pp. 2089-2093, May 1997.

[2] M. Hsieh and C. Wei, "Channel estimation for OFDM systems based on comb-type pilot arrangement in frequency selective fading channels" in *IEEE Trans. Consumer Electron.*, vol.44, no. 1, pp. 217-225, Feb. 1998.

[3] S. Coleri, M. Ergen, A. Puri and A. Bahia, "Channel estimation techniques based on pilot arrangement in OFDM systems" in *IEEE Trans. Broad.*, vol.48, no. 3, pp. 223-229, Sept 2002.

[4] H. Hijazi and L. Ros, "Analytical analysis of Bayesian Cramer-Rao Bound for dynamical Rayleigh channel complex gains estimation in OFDM systems" in *IEEE Trans. Signal Processing*, vol. 57, no. 5, pp. 1889-1900, May 2009.

[5] W. Chen and R. Zhang, "Kalman filter Channel estimator for OFDM systems in time and frequency-selective fading environment" in *Proc. IEEE ICASSP*, vol. 4, pp. 17-21, Montreal, Canada, May 2004.

[6] T.Y. Al-Naffouri, "An EM-based Forward-Backward Kalman Filter for the Estimation of Time-Variant Channels in OFDM" in *IEEE Trans. Signal Processing*, vol. 55, no. 7, pp. 3924-3930, July 2007.

[7] M.S. Sohail, T.Y. Al-Naffouri, "An EM-based frequency domain channel estimation algorithm for multi-access OFDM systems" in *Elsevier Signal Processing*, vol. 90, no. 5, pp. 1562-1572, May 2010.

[8] B. Yang, K. B. Letaief, R. S. Cheng and Z. Cao, "Channel estimation for OFDM transmission in multipath fading channels based on parametric channel modeling" in *IEEE Trans. Commun.*, vol. 49, no. 3, pp. 467-479, March 2001.

[9] N. Chen, J. Zhang, and P. Zhang, "Improved Channel Estimation Based on Parametric Channel Approximation Modeling for OFDM Systems" in *IEEE Trans. Broad.*, vol. 54, no. 2, June 2008.

[10] O. Simeone, Y. Bar-Ness and U. Spagnolini "Pilot-Based Channel Estimation for OFDM Systems by Tracking the Delay-Subspace" in *IEEE Trans. Wireless Commun.*, vol. 3, no. 3, pp. 315-325, January 2004.

[11] H. Hijazi and L. Ros, "Polynomial estimation of time-varying multi-path gains with intercarrier interference mitigation in OFDM systems" in *IEEE Trans. Vehicular Techno.*, vol. 58, no. 1, pp.140-151, January 2009.

[12] H. Hijazi and L. Ros, "Joint Data QR-Detection and Kalman Estimation for OFDM Time-varying Rayleigh Channel Complex Gains" in *IEEE Trans. Commun.*, vol. 58, no. 1, pp. 170-178, January 2010.

[13] K. E. Baddour and N. C. Beaulieu, "Autoregressive modeling for fading channel simulation", in *IEEE Trans. Wireless Commun.*, vol. 4, no. 4, pp. 1650-1662, Jul. 2005.

[14] H. Wang and P. Chang, "On verifying the first-order Markovian assumption for a Rayleigh fading channel model" in *IEEE Trans. Vehicular Techno.*, vol. 45, pp. 353-357, May 1996.

[15] C. Komninakis, C. Fragouli, A.H. Sayed, and R.D. Wesel, "Multi-Input Multi-Output Fading Channel Tracking and Equalization Using Kalman Estimation", in *IEEE Trans. Signal Processing*, vol. 50, no. 5, pp. 1065-1076, May 2002.

[16] P. Banelli, R. Cannizzaro, and L. Rugini,"Data-Aided Kalman Tracking for Channel Estimation in Doppler-Affected OFDM Systems" in *Proc. IEEE ICASSP*, vol. 3, pp. 133-136, Hawaï, USA, April 2007.

[17] H. Abeida, J.M. Brossier, L. Ros and J. Vilà-Valls, "An EM algorithm for path delay and complex gain estimation of a slowly varying fading channel for CPM signals", in *Proc. IEEE Globecom*, pp. 47-52, Hawaï, Dec. 2009.

[18] L. Ros, H. Hijazi and E.P. Simon "Paths Complex Gain Tracking Algorithms for OFDM Receiver in Slowly-Varying Channels" in *Proc. IEEE ISCCSP*, pp. 1-6, Limassol, Cyprus, March 2010.

[19] WC Lindsey, CM Chie, "A survey of digital phase-locked loops" in *Proceedings of the IEEE*, vol. 69, no. 4, p. 410-431, Apr. 1981.

[20] A. Patapoutian, "On phase-locked loops and Kalman filters" in *IEEE Trans. Commun.*, vol. 47, pp. 670672, May 1999.

[21] G. S. Christiansen, "Modeling of a PRML timing loop as a Kalman filter, in *Proc. IEEE Globecom*, vol. 2, pp. 1157-1161, 1994.

[22] E. Simon, L. Ros and K. Raoof, "Synchronization over rapidly time-varying multipath channel for CDMA downlink RAKE receivers in Time-Division mode", in *IEEE Trans. Vehicular Techno.*, vol. 56. no. 4, pp. 2216 - 2225, Jul. 2007.

[23] R. Winkelstein, "Closed Form Evaluation of Symmetric Two-Sided Complex Integrals", in *TDA Progress Report*, no. 42-65, pp. 133-141, July and August 1981.

[24] W. C. Jakes, *Microwave Mobile Communications.* IEEE Press, 1983.

[25] H.G. Myung, D.J. Goodman, *Single Carrier-FDMA. A new air interface for long term evolution.* Wiley, 2008.

[26] U. Mengali, A.N. D'Andrea, *Synchronization Techniques for Digital Receivers (Applications of Communications Theory).* PLENUM, 1997.

[27] F.M. Gardner, *Phaselock Techniques.* Wiley, 2nd edition, 1979.

[28] B. Porat, *A course in digital signal processing.* Wiley, 1997.

[29] E.I. Jury, *Theory and Application of the Z-Transform Method.* Wiley, New York, 1964.

[30] S.M. Kay, *Fundamentals of Statistical Signal Processing: Estimation Theory.* Prentice Hall PTR, 1993.

[31] B.D.O. Anderson and J.B. Moore, *Optimal Filtering.* Englewood Cliffs, 1979.